Shear resistance of composite steel concrete plate girder decks

Sérgio Marcelo de Deus Nascimento
sergio.nascimento@tecnico.ulisboa.pt

Abstract

Steel-concrete composite bridge decks combine the best characteristics of each component material, leading to an optimize cost/resistance ratio of the structure. This is a very competitive solution because it is formed by different prefabricated parts, making construction faster and assuring its high quality.

In this dissertation, the resistance of slender plate girders with the I-shape subjected to shear loading is studied, first when these beams are inserted in a steel structure, and then evaluating the case in which a reinforced concrete slab is connected to the top flange of the plate girder.

Thus, in order to evaluate the ultimate strength of a slender steel plate girder, the plate buckling phenomenon due to shear stress is investigated through four different models proposed in the last 50 years, taking into account the post-critical resistance. The results obtained by these models are compared with the different experimental results obtained in the literature.

This study is extended to the evaluation of the ultimate capacity of composite plate girders, presenting two models for this case and comparing the results with the few existing laboratory test results.

The different models of analysis are applied to a case study – a steel-concrete composite bridge recently constructed in Equatorial Guinea, evaluating for each model the shear strength, and evidencing the contribution of the reinforced concrete slab.

Key-words: Steel-concrete composite bridge; Plate girder; Pure shear; Plate buckling; Post-critical shear resistance.

1. Introduction

During the years, composite bridges that combine steel plate girders with a concrete slab deck have been widely used due to their economic, constructive and structural advantages. A composite steel-concrete bridge mobilizes the best mechanical characteristics of both structural materials.

The present work specifically addresses the case of bridges in which the steel girder has an I-shaped welded section where the concrete slab of pavement is attached to the upper flange. The two acting together provides stiffness and resistance to the applied bending moments and axial force acting on the deck. Its application extends from short to medium span to long span pedestrian, road and railway bridges.

In accordance with the current design codes, composite plate girders must be design to shear assuming the independent behaviour of the steel girder and the concrete slab. And usually disregarding any contribution that may exist by the reinforced concrete slab. This assumption, on the safety side, may lead to the oversizing of these steel plate girders to shear.

2. Slender plate girders

2.1 Examples

There are several examples of important structures in which the plate girders were used in Portugal, such as the *Alcântara* railway viaduct in Lisbon. Completed in 1998, this deck allows rail access to the *25 de Abril* bridge to cross over the *Tejo* river, as shown in Figure 1 (a) [1] [2]. The cover of the *Dragão* stadium in Oporto (Figure 1 (b) [3]), built in 2003, is also a relevant example of steel plate girders applied to large span roofs. The new railway bridge over the *Sado* river and the respective access viaducts, in Figure 1 (c), known as the *Alcácer do Sal* variant, completed in 2012, is another example of a long viaduct where composite plate girders were widely used, among many others in Portugal [4]. In addition, the use of steel plate girders at international level has a very relevant expression, particularly in steel-concrete plate girders decks and large span roofs.

(a) (b)

(c)

Figure 1 – Examples of steel plate girders structures built in Portugal

2.2 Design rules

Some basic design rules are introduced to pre-design the steel plate girder according to some references.

- **Girder height h (and web height d)**

The height h of the plate girder is function of the bridge span L. However, the L/h ratio must also take into account the loading, support type and the steel grade adopted. Thus, the slenderness is usually the following values [5], [6]:

- ✓ Industrial building L_e/h from 15 to 25
- ✓ Road bridges L_e/h from 12 to 18
- ✓ Railway bridges L_e/h from 10 to 15
- ✓ Heavy crane L_e/h from 7 to 12

where L_e stands for an equivalent span of the structure. The web height d is obtained subtracting the flanges thickness t_f to the girder height h .

- **Web thickness t_w**

The web thickness is designed to satisfy requirements of shear resistance, fatigue and steel corrosion resistance. The web thickness is usually comprehended between 8 and 20 mm. The web slenderness is also defined from 100 (without stiffeners) to 300 (with stiffeners), being usual to take values from 100 to 200 [6], [7].

- **Flange width b_f and thickness t_f**

The flange width b_f design on based on the stiffness and resistance criteria. This is commonly taken in the range from $h/5$ to $h/3$ but less than 1000 mm, being able to reach lower values in case of a composite compression flange. Multiples of 25 mm are often used for constructive ease [5], [6].

The flange thickness t_f, if under tensile stress, is acceptable to be between 12 and 60 mm. If subjected to compression stress, its slenderness should be limited to 30ε (with $\varepsilon = \sqrt{235/f_y}$) to avoid local buckling [6], [7].

- **Transversal stiffeners**

Due to slender web plate's use, transversal stiffeners are recommended in order to reduce the size of the web and increase significantly its strength. The spacing between transverse stiffeners, a, is generally taken between $1.0d$ and $1.5d$ [7].

3. Shear resistance of plate girders

Although the post-critical behaviour of thin plates was identified by Wilson in 1886 and studied by Wagner which concluded the diagonal field tension theory in 1929, until the 60's of the last century the web plates were designed to its critical resistance. However, it was in 1959 that several studies were carried out by Basler and Thurlimann on the post-critical behaviour. Based on these a method was proposed by them to design the web plates taking into account its post-critical resistance, related to the post-bucking behaviour. In the following decades, several models were proposed in order to approximate the models results to the experimental ones obtained in laboratory [8]. Followed by Rockey and Skaloud in 1969, the Cardiff model was proposed which proved to be adjusted to the experimental results [9]. In 1972 Dubas developed the simple post-critical method, which alongside with the Cardiff model formed the base of ENV 1993-1-1 (1992) [10]. In 1998, a simpler method was proposed, by recalibrating the Höglund method (1975); this method was introduced in the current version of the EC3-1-5 [11].

The pre-critical phase of a plate occurs before buckling. At this stage the plate is subjected to a pure shear stress state with tensions and compressions occurring with the same intensity, at 45° with the panel corners (Figure 2 (a)). Exceeded the critical resistance, local plate buckling occurs. However, this does not represent the failure of the girder. A resistance reserve is mobilized, associated to a change of the direction of the tensile field action. This field loses the capacity to withstand normal stresses in the direction of the compression stresses, yet normal tensile stresses may increase until the yield stress is reached (Figure 2 (b)).

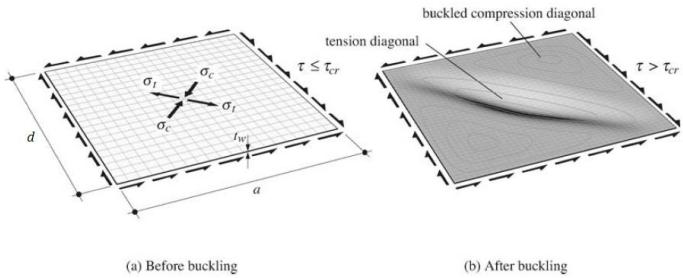

Figure 2 – Buckling of a panel in shear. Adapted from [12]

Therefore, the critical contribution is calculated using linear elastic buckling theory and is given by eq. (1):

$$V_{cr} = \tau_{cr} \cdot d \cdot t_w \tag{1}$$

where the critical shear stress τ_{cr} is:

$$\tau_{cr} = k_\tau \cdot \frac{\pi^2 \cdot E}{12 \cdot (1-\nu^2)} \cdot \left(\frac{t_w}{d}\right)^2 \tag{2}$$

The buckling coefficient k_τ is function of the slenderness a/d and for a simple supported panel is given by:

$$k_\tau = 4.0 + \frac{5.34}{(a/d)^2} \qquad \text{if } {}^{a}/_{d} \leq 1 \qquad (3)$$

$$k_\tau = 5.34 + \frac{4.0}{(a/d)^2} \qquad \text{if } {}^{a}/_{d} > 1 \qquad (4)$$

3.1 Basler model (M1)

In this model, it is assumed that the diagonal field can only be formed if the boundary conditions allow it. Basler model assumes that the stiffness of the flange is very small, considering it flexible. As consequence, the diagonal can only be anchored in the next panel through the transverse stiffeners, which are admitted as rigid (Figure 3). Thus, the ultimate shear resistance according to Basler is given, in a simplified way, by:

$$V_R = V_{cr} + V_\sigma = \left(\tau_{cr} + \frac{\sqrt{3}\cdot(\tau_{yw} - \tau_{cr})}{2\cdot\sqrt{1 + a/d^2}}\right)\cdot d \cdot t_w \qquad (5)$$

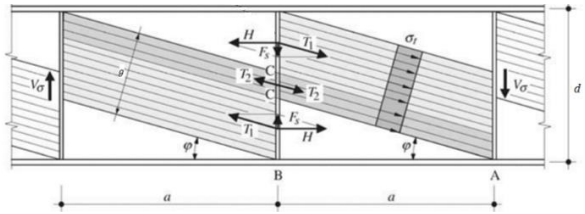

Figure 3 – Basler Model scheme. Adapted from [12]

So, applied to the case study (section in Figure 4) with a=2535 mm, steel grade S355 NL and Young Modulus E=210 GPa, results V_R = 5 474.5 kN.

Figure 4 – Cross section of case study

3.2 Tension field method (M2)

Based on the Cardiff model this method is applies to stiffened girders with $1<a/d<3$. This tension field is anchored not only in the top and bottom flanges but also in the transverse stiffeners (Figure 5). Thus, all elements are classified as rigid by the tension field method. The transmission of loads mechanism after buckling can be related with a Pratt truss.

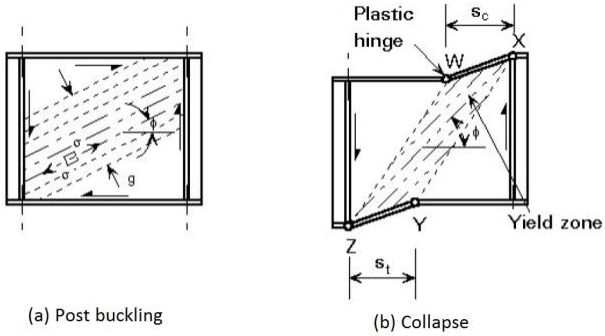

Figure 5 – Tension Field Method scheme. Adapted from [6]

Thereby, the ultimate shear strength is given by:

$$V_{bb,Rk} = d \cdot t_w \cdot \tau_{bb} + 0.9 \cdot g \cdot t_w \cdot \sigma_t \cdot \sin\varphi \qquad (6)$$

The τ_{bb} have the same physical meaning as τ_{cr}, but is defined through equations (7), (8) and (9), depending on the normalized slenderness $\bar{\lambda}_w$ ($\bar{\lambda}_w = \sqrt{\tau_y/\tau_{cr}}$). The tension carried by the buckled membrane σ_t is given by the Von Mises-Hencky, in a simplified way by eq. (10).

$$\tau_{bb} = \frac{f_{yw}}{\sqrt{3}} \qquad \bar{\lambda}_w \leq 0.8 \qquad (7)$$

$$\tau_{bb} = \left[1 - 0.8\cdot(\bar{\lambda}_w - 0.8)\right]\cdot\frac{f_{yw}}{\sqrt{3}} \qquad 0.8 < \bar{\lambda}_w < 1.25 \qquad (8)$$

$$\tau_{bb} = \left(\frac{1}{\bar{\lambda}_w^{\,2}}\right)\cdot\frac{f_{yw}}{\sqrt{3}} \qquad \bar{\lambda}_w \geq 1.25 \qquad (9)$$

$$\sigma_t = \sqrt{3}\cdot(\tau_{yw} - \tau_{cr}) \qquad (10)$$

The width of the tension field g may be calculated based on the collapse mechanism of Figure 5 (b), with the formation of four plastic hinges, given by eq. (12). Thus, this value depends distance between the plastic hinges at the compression and tension flanges, C_c and C_t, which may be obtained by eq. (11).

$$C = \frac{2}{\sin\varphi}\cdot\sqrt{\frac{M_{Nf,Rk}}{t_w\cdot\sigma_t}} \leq a \qquad (11)$$

$$g = d\cdot\cos\varphi - (a - C_c - C_t)\cdot\sin\varphi \qquad (12)$$

The tension field angle φ should be iterated in order to maximize the shear resistance. This angle must be between $\theta/2<\varphi<\theta$, where θ related to the panel diagonal inclination. As a first approximation $\varphi = \theta/1.5$ is recommended [6].

Applied to the case study and knowing that the axial stress acting on the girder is 8 898.3 kN (in order to reduce the $M_{f,Rk}$), the ultimate shear strength is V_R = 5 388.7 kN for φ=23.9°.

3.3 Simple post-critical method (M3)

This method is applicable both to stiffened and non-stiffened plate girders, which gives it large applicability. However, it is normally considered to be the most conservative method [10]. The ultimate shear strength is given simply by:

$$V_{ba,Rk} = d \cdot t_w \cdot \tau_{ba} \qquad (13)$$

Again, the τ_{ba} parameter is defined through equations (14), (15) and (16) depending on the normalized slenderness.

$$\tau_{bb} = \frac{f_{yw}}{\sqrt{3}} \qquad \bar{\lambda}_w \leq 0.8 \qquad (14)$$

$$\tau_{bb} = \left[1 - 0.625 \cdot (\bar{\lambda}_w - 0.8)\right] \cdot \frac{f_{yw}}{\sqrt{3}} \qquad 0.8 < \bar{\lambda}_w < 1.2 \qquad (15)$$

$$\tau_{bb} = \left(\frac{0.9}{\bar{\lambda}_w^{\,2}}\right) \cdot \frac{f_{yw}}{\sqrt{3}} \qquad \bar{\lambda}_w \geq 1.2 \qquad (16)$$

Applying the simple post-critical method to the case study one obtains V_R = 4 879.3 kN as the ultimate shear resistance of the steel plate girder.

3.4 Rotated stress field method (M4)

The need of a simpler method, capable of evaluating also the strength of non-stiffened and longitudinal stiffened plate girders, led to the adoption by the EC3-1-1 [13] of the Höglund method, now called rotated stress field method. In one hand, along with this method adequate precision is a large applicability allowing the determination of the resistance in web panels with any distance between transverse stiffeners. In other hand, this method is not quite explicit defining the pre-critical and post-critical portions.

Based on this method, the ultimate shear strength is defined by:

$$V_{b,Rd} = V_{bw,Rd} + V_{bf,Rd} \leq V_{plw,Rd} \qquad (17)$$

Where the web contribution is given by:

$$V_{bw,Rd} = \frac{\chi_w \cdot d \cdot t_w \cdot f_{yw}/\sqrt{3}}{\gamma_{M1}} \qquad (18)$$

The reduction factor of the web χ_w is defined by the Table 1. Note that in very thick webs, and until steel grade S460, the failure occurs with a shear stress 20% higher than $f_{yw}/\sqrt{3}$ [9], which is taken into account by using η = 1.0 to 1.2, when $\bar{\lambda}_w < 0.83/\eta$.

Table 1 – Reduction factor according to M4

$\bar{\lambda}_w = \sqrt{\frac{f_{yw}/\sqrt{3}}{\tau_{cr}}}$	Rigid Panel	Non-rigid Panel
$\bar{\lambda}_w < 0.83/\eta$	η	η
$0.83/\eta \leq \bar{\lambda}_w < 1.08$	$0.83/\bar{\lambda}_w$	$0.83/\bar{\lambda}_w$
$\bar{\lambda}_w \geq 1.08$	$1.37/(0.7+\bar{\lambda}_w)$	$0.83/\bar{\lambda}_w$

The flange contribution despite being usually small compared to the web contribution, it still exists. It is associated to the formation of four plastic hinges in the compression and tension flange at the distance c from the transverse stiffeners. This contribution is given by:

$$V_{bf,Rd} = \frac{b_f \cdot t_f^{\,2}}{c} \cdot \frac{f_{yf}}{\gamma_{M1}} \cdot \left[1 - \left(\frac{M_{Ed}}{M_{f,Rd}}\right)^2\right] \qquad (19)$$

$$c = a \cdot \left(0.25 + \frac{1.6 \cdot b_f \cdot t_f^{\,2} \cdot f_{yf}}{t_w \cdot d^2 \cdot f_{yw}}\right) \qquad (20)$$

Where $M_{f,Rd}$ is given by eq. (21), which might be further reduced by the presence of applied normal forces.

$$M_{f,Rd} = \frac{b_f \cdot t_f \cdot f_{yf} \cdot d}{\gamma_{M0}} \qquad (21)$$

Using this method to evaluate the shear resistance of one girder of the case study and knowing that the applied bending moment is M_{Ed} = -16017 kNm, the ultimate shear resistance is V_R = 4 658.9 kN, disregarding the flange contribution

4. Comparison with experimental tests

In order to validate the models M1, M2, M3 and M4, their results are compared with experimental values. The test campaigns who these results are used were:

1) Test 1 (T1)

Eng. Carlos Gomes from University of Minho (Portugal), in 1999 he tested seven different steel plate girders and one steel-concrete composite one in his MsC research [14]. Table 2 defines geometries and material proprieties of the steel girders tested. The yield tension is the same for both flanges and the web.

Table 2 – Dimensions and material properties of T1 steel girders

G	d (mm)	a (mm)	a/d	t_w (mm)	t_f (mm)	b_f (mm)	f_y (MPa)	E_w (GPa)
V1	300	1800	6.0	2.0	5	100	275	207
VT1	300	900	3.0	2.0	5	100	275	207
VT2	300	600	2.0	2.0	5	100	275	207
VT3	300	300	1.0	2.0	5	100	275	207

Table 3 presents the model shear resistances as well as the experimental results.

Table 3 – Experimental and model results for T1 steel girders

G	a/d	$V_{experimental}$ (kN)	V_{model}				Failure Mode
			V_{M1} (kN)	V_{M2} (kN)	V_{M3} (kN)	V_{M4} (kN)	
V1	6.0	35.0	36.9	NA	45.8	52.2	Local buck.
VT1	3.0	55.0	47.0	42.6	47.2	54.7	Shear buck.
VT2	2.0	55.0	56.3	50.8	49.4	57.8	Shear buck.
VT3	1.0	75.0	76.4	73.1	60.0	69.7	Shear buck.

Girder V1 has only transverse stiffeners in the supports, and not in the application load zone, leading to failure due to local buckling of the web instead of web buckling. Due to this fact, the (a/d) ratio is 6, outside the range between 1 and 3, which means that the tension field method in not applicable.

For (a/d) rations equal or less than 2, a common value in practice, all models except the simple post-critical method (M3) have good estimation of the results. However, increasing this ratio the model that better suits is the rotated stress field method (M4). As expected, the plate girder strength increases as the (a/d) ratio decreases, meaning shorter distance a between stiffeners that means a larger number of stiffeners.

According to the Figure 6, the most accurate model is the M4. The M3 Is the one that most underestimates the girder

shear capacity, where all calculated resistances values were much lower than the actual strength of the tested girders.

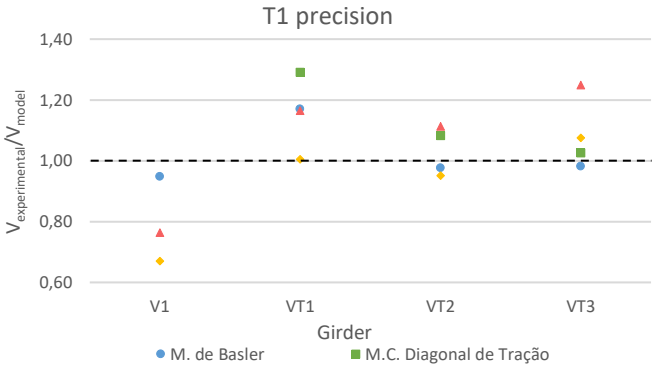

Figure 6 – Precision of models for T1 steel girders

2) Test 2 (T2)

In 1999, Sung C. Lee and Chai H. Yoo from University of Dongguk (South Korea) and Auburn University (USA) led an investigation testing ten steel plate girders to validate their model [15]. In the Table 4 the girders studied are introduced, and for all specimens f_{yf} = 303.8 MPa.

Table 4 – Dimensions and material properties of T2 steel girders

G	d (mm)	a (mm)	a/d	t_w (mm)	t_f (mm)	b_f (mm)	f_{yw} (MPa)	E_w (GPa)
G1	400	400	1.0	4.0	15	130	318.5	204
G2	600	600	1.0	4.0	10	200	318.5	204
G3	600	600	1.0	4.0	15	200	318.5	204
G4	400	600	1.5	4.0	15	130	318.5	204
G5	600	900	1.5	4.0	10	200	318.5	204
G6	600	900	1.5	4.0	20	200	318.5	204
G7	600	1200	2.0	4.0	10	200	285.2	204
G8	600	1200	2.0	4.0	15	200	285.2	204
G9	400	1200	3.0	4.0	10	130	293.0	204
G10	400	1200	3.0	4.0	15	130	293.0	204

Table 5 resumes models and experimental results.

Table 5 – Experimental and model results for T2 steel girders

G	a/d	$V_{experimental}$ (kN)	V_{model}				Faiure Mode
			V_{M1} (kN)	V_{M2} (kN)	V_{M3} (kN)	V_{M4} (kN)	
G1	1.0	282.4	266.1	299.3	251.3	294.2	Shear buck.
G2	1.0	332.5	341.5	318.5	256.3	306.1	Shear buck.
G3	1.0	337.4	341.5	348.0	256.3	345.3	Shear buck.
G4	1.5	268.8	250.4	265.5	223.7	260.3	Shear buck.
G5	1.5	286.4	284.7	253.5	223.7	269.1	Shear buck.
G6	1.5	312.8	284.7	304.7	223.7	324.9	Shear buck.
G7	2.0	258.9	229.5	206.7	199.8	236.8	Shear buck.
G8	2.0	276.5	229.5	225.7	199.8	255.9	Shear buck.
G9	3.0	161.8	198.0	197.9	193.4	200.8	Bending
G10	3.0	194.6	198.0	207.2	193.4	212.0	Bend. and buck.

Based on Figure 7, the most accurate model to predict the girder's shear capacity is again the M4. Once more M3 is the one that most underestimates the girder's strength. Also, the excellent results obtained by models M1 and M2 for a/d ratios under 1.5.

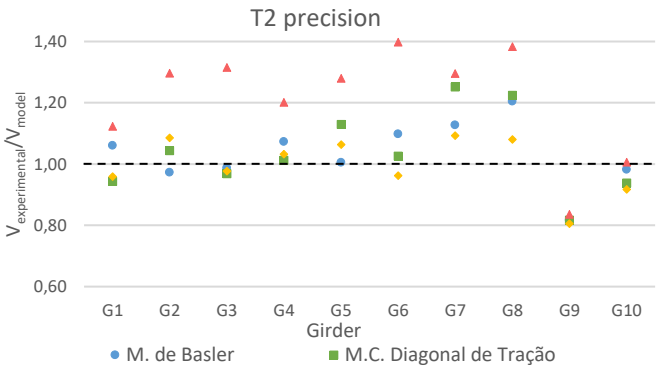

Figure 7 – Precision of models for T2 steel girders

3) Test 3 (T3)

In 2003, N. E. Shanmugam and K. Baskar, from National University of Singapore (Singapore Republic) developed an extensive experimental test campaign where the main goal was to study the influence of the concrete slab on the ultimate strength of the plate girder [16]. Table 6 introduces the girders studied.

Table 6 – Dimensions and material properties of T3 steel girders

G	d (mm)	a (mm)	a/d	t_w (mm)	t_f (mm)	b_f (mm)	$f_{yf,t}$ (MPa)	$f_{yf,b}$ (MPa)	f_{yw} (MPa)	E_w (GPa)
SPG1	750	1141	1.52	3.0	20	200	272	273	286	202
SPG2	750	1141	1.52	5.0	20	260	300	292	275	202

In Table 7 both the model results and the experimental values are presented.

Table 7 – Experimental and model results for T3 steel girders

G	a/d	$V_{experimental}$ (kN)	Plate Borders	V_{modelo}				Failure Mode
				V_{M1} (kN)	V_{M2} (kN)	V_{M3} (kN)	V_{M4} (kN)	
SPG1	1.52	244.0	Simply Sup.	202.9	202.3	118.9	204.5	Shear buck.
			Fixed	217.9	221.2	150.9	234.4	
SPG2	1.52	402.5	Simply Sup.	396.0	406.5	322.1	432.0	Shear buck.

Note that, for the SPG1 the model results are quite different from the experimental results. However, noticing that t_w=3 mm welded to 20 mm thick flanges and 16 mm thick transverse stiffeners, the assumption of obtaining the critical load with simply supported panel model may not be close to reality. Due this fact, the panel shear strength was reassessed considering the panel fixed, founding model results closer to the experimental ones.

According to Figure 8, the most accurate model is M4 alongside with M2.

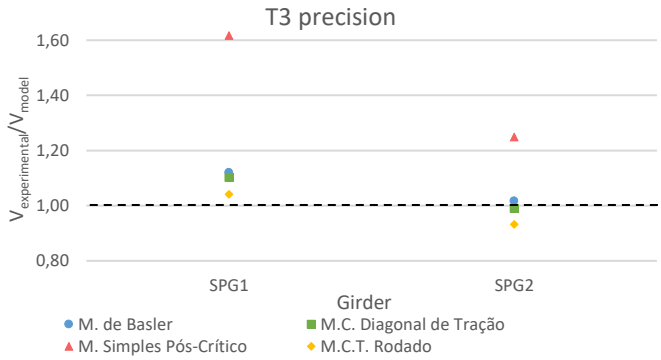

Figure 8 – Precision of models for T3 steel girders

Some conclusions about the four different models studied are summarised:

• Despite being developed in the 60s and the simplifications assumed for its use, M1 is shown to be an accurate in order to predict the shear resistance of a plate girder. The average accuracy, measured by $V_{experimental}/V_{model}$, is 1.06.

• The M2 is also a quite accurate method, with an average score of 1.08. Although the complexity associated to the iterative calculation of the tension field inclination makes its applicability more difficult.

• Although being very simply to use, the M3 is by far the method that most underestimates the girder capacity to shear loading. Its average precision is 1.28.

• Finally, the M4, currently used by EC3-1-5 [11], combining the simplicity of calculation and large applicability, provides very close results to the experimental tests, being the most accurate model, with a ratio of 1.02 between the $V_{experimental}/V_{model}$. These ratios for the three tests are resumed in Figure 9.

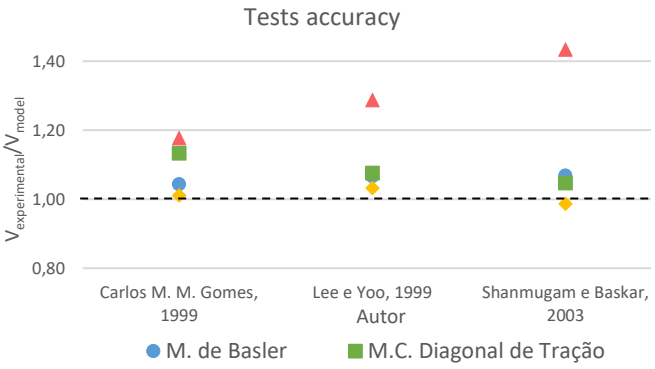

Figure 9 – Average accuracy of each model

5. Composite steel-concrete contribution to shear resistance of plate girders

In bridges and building floors, plate girders support pavements formed by reinforced concrete slabs. Despite the fact that the plate girder is connected to a concrete slab through studs welded to the girder's top flange which makes the girder capable to resist to higher shear loading, this composite actions is currently ignored in design codes [17].

Few studies have investigated the behaviour of composite plate girders under bending and shear loading. In 1982, Allison et al. conducted an experimental investigation for both bending and shear loading proposing some equations to predict the ultimate resistance of these girders [18]. Experimental studies by Porter and Cherif in 1987 [19] were followed by Narayanan et al. in 1989 [20] and Roberts and Al-Amery in 1991 testing composite plate girders with rectangular openings in the web, concluding that the shear connectors give the fundamental contributions to ensure the composite action [21]. Later in 2003, Shanmugam and Baskar [16] continued studies previously conducted in 2003, proposing in 2012 a method to predict the shear strength of composite plate girders [22], [23]. Recently, in 2015, Yatim, Shanmugam and Wan Badaruzzaman also proposed a method [24].

The composite plate girder may be considered to undergo four phases of load carrying mechanism, as shown in Figure *10*. In the first two stages (a) and (b), compressive and tensile principal stresses are developed and a new load carrying mechanism is formed within the plate, any additional shear loading is carried by an inclined tensile membrane stress field. After lateral buckling the web will reach yield stress on the membrane ABCD, where the plastic hinges are formed in the top and bottom flange, related to stage (c). The tension field is partly anchored to the concrete slab through composite action which gives rise to stronger flange action in compression compared to tension side. Due this fact the distance between plastic hinges in the compression flanges C_c is larger than that in the tension flange C_t. This results in larger load carrying capacity compared to steel girder acting alone. Final failure of the girder will occur with the formation of the plastic hinges and extensive cracking in the slab. Ultimate shear capacity of the composite plate girders may be considered as combined strength resisted by steel part of the girder V_s and by the concrete slab V_c [23].

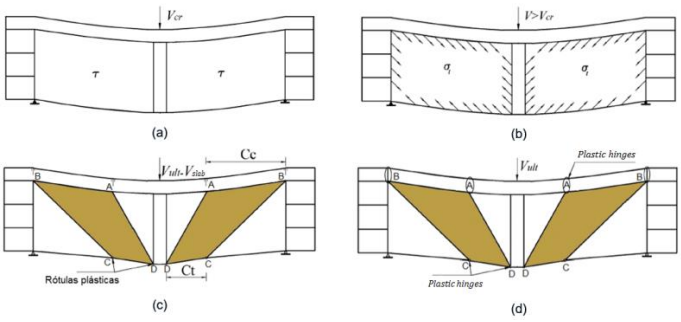

Figure 10 – Four phases of load carrying mechanism in a web panel. Adapted from [23]

5.1 Model 1 (ML1)

According to Shanmugam and Baskar [22] the shear strength of the steel plate girder V_s may be calculated using a similar approach to the Cardiff model [25], by:

$$V_s = \tau_{cr} \cdot d \cdot t_w + \sigma_t \cdot g \cdot t_w \cdot \sin\varphi \quad (22)$$

The distance between plastic hinges on the compressed flange may be calculated by eq. (11) where the plastic moment of the composite compression flange M_{pn} must be considered, as shown in Figure 11. The tension carried by the buckled membrane σ_t is given by the Von Mises-Hencky.

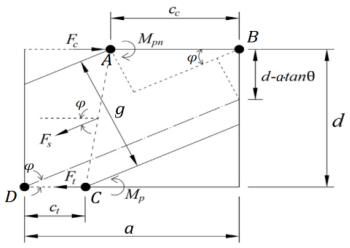

Figure 11 – Equilibrium of forces acting in post-buckled web. Adapted from [24]

The concrete slab contribution depends upon the connection between the steel girder and the concrete slab. The shear studs are shown to be the primarily responsible for sustaining the composite action. The tensile force transferred from the plate girder to concrete slab by means of these shear connectors cause shear failure of concrete in two successive studs. Finite element analyses on composite plate girders have also shown such behaviour. The manner in which shear failure occurs varies widely depending on the arrangement, spacing and size of the studs.

The shear strength of concrete slab V_c is based on a strut and tie model, similar to the one used in the design of deep beams, where it can be used to model the internal forces in the concrete slab. Dividing the concrete slab in B-region and D-region, V_c may be given by the sum of the two parts calculated by eq. (23) and (24) [22].

$$V_c^B = F_{st} \cdot \sin\omega \cdot N_{st} \quad (23)$$

$$V_c^B = 0.17 \cdot \sqrt{f'_c} \cdot (b_s - b_f) \cdot d_s \quad (24)$$

Finally, the ultimate shear resistance of the composite girder is given by:

$$V_R = V_s + V_c \quad (25)$$

5.2 Model 2 (ML2)

According to Yatim, Shanmugam and Wan Badaruzzaman, the shear resistance of the steel plate girder V_s may be given by eq. (22). Moreover, the shear strength of the concrete slab V_c is given by:

$$V_c = V_a + \xi \cdot (V_b - V_a) \quad (26)$$

Where V_a is the shear resistance of the concrete slab alone, according to EC2-1-1 [26], V_b the shear resistance of the concrete slab fully connected to the steel plate girder given by the pull-out capacity of the headed stud connectors given by equations (27) and (28) [24]. Finally, the ξ is the degree of interaction according to EC4-2 [27], [28].

$$V_b = [\pi \cdot (D_n + h_n) + 2 \cdot s] \cdot h_n \cdot f_{ctm} \quad \text{For pair studs} \quad (27)$$

$$V_b = \pi \cdot (D_n + h_n) \cdot h_n \cdot f_{ctm} \quad \text{For single stud} \quad (28)$$

5.3 Comparison with experimental tests

1) Composite Test 1 (CT1)

The first steel-concrete composite experimental test studied on the current paper was carried by Eng. Carlos Gomes from University of Minho (Portugal) in 1999, where in addition to the seven steel plate girder tested, one composite was loaded until failure [14].

The girder dimensions are similar to V1 from Test 1 in Cap. 4. The non-reinforced concrete slab had a C45 grade with b=500 mm, h_s=60 mm where the stud connectors had the head diameter D_n=18 mm, height h_n=40 mm in a single row (N_{st}=1) spaced 100 mm. It was assumed that ξ=1. Thus, the experimental and model results are in Table 8.

Table 8 – Experimental and model results for CT1 composite girders

Girder	$V_{experimental}$ (kN)	V_{M4} (kN)	V_{ML1} (kN)	V_{ML2} (kN)	$V_{experimental}/V_{ML1}$	$V_{experimental}/V_{ML2}$
VT1M	73.0	54.7	71.0	71.8	1.03	1.02

The ultimate shear resistance for the VT1M composite girder tested was 73 kN, 33% higher than the 55 kN achieved in V1 steel girder test. This increase evidences the compressed slab contribution to the shear resistance.

It is also possible to conclude that models ML1 and ML2 does a good evaluation with a $V_{experimental}/V_{ML}$ ratio of 1.03 and 1.02.

2) Composite Test 2 (CT2)

The second experimental test was carried by N. E. Shanmugam and K. Baskar, from National University of Singapore, in 2003, introduced in Test 2 of Cap. 4 [16]. The steel plate girder of CPG1 and CPG3 has the same characteristics as SPG1 introduced in T3, Cap. 4. The same applies to CPG2 and CPG4 where the steel plate girder characteristics are the same as SPG2. Table 9 defines concrete slab and shear connectors data. Note that the difference between CPG1 and CPG3 is not only the concrete grade but also the use of shear reinforcement in the second test, known as shear link as described in [16]. The same applies to CPG2 and CPG4.

Table 9 – Concrete slab data for CT2 composite girders

Girder	h_s (mm)	b_s (mm)	f_{ck} (MPa)	f_{ctm} (MPa)	D_n (mm)	h_n (mm)	l (mm)	s (mm)	N_{st}
CPG1	150	1000	40.2	3.0	32	100	155	155	2
CPG3	150	1000	45.9	3.7	32	100	155	155	2
CPG2	150	1000	41.9	3.0	32	100	155	155	2
CPG4	150	1000	45.0	3.7	32	100	155	155	2

From Table 7 (Steel plate girders) and Table 10 (Concrete plate girders) is possible to evaluate the concrete slab contribution to shear strength by comparison of experimental results. It is concluded that this contribution is significant,

being 77% from SPG1 to CPG1 and 39% from SPG2 to CPG2 (even without shear link reinforcement).

Table 10 – Experimental and model results for CT2 composite girders

Girder	$V_{experimental}$ (kN)	V_{M4} (kN)	V_{ML1} (kN)	V_{ML2} (kN)	$V_{experimental}/V_{ML1}$	$V_{experimental}/V_{ML2}$
CPG1	430.5	234.4	437.4	437.2	0.98	0.98
CPG3*	542.5	234.4	446.6	487.9	1.21	1.11
CPG2	562.0	432.0	658.1	644.3	0.85	0.87
CPG4*	675.0	432.0	662.8	695.0	1.02	0.97

For CT2 test (without shear link), models ML1 and ML2 have an average precision of 0.92 and 0.93, leading to good results despite not being in the safety side.

3) Composite Test 3 (CT3)

Recently in 2015, Yatim, Shanmugam and Wan Badaruzzaman carried experimental tests on eight steel-concrete composite plate girders in order to study the influence of the connectors on the ultimate shear resistance of the composite girder.

The steel girder characteristics, such as dimensions and materials properties, might be found in reference [24]. The web height d=750 mm with t_w=3 mm and a=884.75 mm. Flanges are 20 per 200 mm.

The concrete and shear connector's characteristics are presented in Table 11.

Table 11 – Concrete slab data for CT3 composite girders

Girder	h_s (mm)	b_s (mm)	f_{ck} (MPa)	f_{ctm} (MPa)	D_n (mm)	h_n (mm)	l (mm)	s (mm)	N_{st}	ξ
G1C20	150	1000	19.7	2.0	32	103	135	80	2	1.0
G1C30	150	1000	31.7	2.4	32	103	135	80	2	1.0
G2C30	150	1000	33.3	2.9	32	103	279	80	2	0.5
G3C30	150	1000	27.2	1.9	32	103	465	80	2	0.3
G4C20	150	1000	30.1	2.5	32	103	465	80	2	0.1
G4C30	150	1000	35.5	2.3	32	103	465	0	1	0.1
G5C30	150	1000	28.9	2.1	29	85	116	0	1	0.8
G6C30	150	1000	35.9	2.0	40	116	465	80	2	0.5

Table 12 – Experimental and model results for CT3 composite girders

Girder	$V_{experimental}$ (kN)	V_{M4} (kN)	V_{ML1} (kN)	V_{ML2} (kN)	$V_{experimental}/V_{ML1}$	$V_{experimental}/V_{ML2}$
G1C20	387.5	255.7	494.2	405.4	0.78	0.96
G1C30	414.0	242.8	511.0	416.5	0.81	0.99
G2C30	373.5	227.3	486.8	381.9	0.77	0.98
G3C30	343.5	243.2	489.9	356.9	0.70	0.96
G4C20	311.5	227.4	466.0	331.6	0.67	0.94
G4C30	315.5	235.0	484.7	342.5	0.65	0.92
G5C30	392.5	237.9	496.8	355.7	0.79	1.10
G6C30	377.5	240.6	502.7	385.4	0.75	0.98

According to Table 12 and comparing M4 results with experimental values it is possible to conclude that the higher slab contribution occurs for G1C30 which represents a shear resistance increase about 71%.

In one hand, it is possible to conclude that the model ML1 appears not to be very accurate for this experimental tests, as it always overestimates the test results. In the other hand, the M2 does an excellent evaluation of the composite girder strength with an average score of 0.98.

4) Composite Test 4 (CT4)

Finally, experimental test carried by Blanc and Navarro in 1999 in EPFL (Switzerland) on two different composite girders had the main goal of study the influence of the concrete slab on girders shear resistance under hogging bending moment [29]. The plate girders are introduced in Table 13.

Table 13 – Dimensions of specimens CT4 composite girders

G	d (mm)	a (mm)	a/d	t_w (mm)	$t_{f,t}$ (mm)	$b_{f,t}$ (mm)	$t_{f,b}$ (mm)	$b_{f,b}$ (mm)
F1P3	800	1200	1.50	6	10	160	15	200
F1P5	800	1800	2.25	6	10	160	15	200
F2P1	800	1200	1.50	6	10	160	15	200

Note that the f_{yw}=393 and 394 MPa for F1 and F2 girders. The yield tension of the top flange is $f_{yf,t}$=378 and 392 MPa for F1 and F2 girders. The yield tension of the bottom flange is $f_{yf,b}$=353 MPa for both F1 and F2 composite girders. Finally, Young Modulus of the web steel is 202 GPa. In Table 14 the concrete slab characteristics are introduced.

Table 14 – Concrete slab data for CT4 composite girders

G	h_s (mm)	b_s (mm)	f_{ck} (MPa)	f_{ctm} (MPa)	D_n (mm)	h_n (mm)	l (mm)	s (mm)	N_{st}
F1P3	140	800	40	2.5	32	125	150	80	2
F1P5	140	800	40	2.5	32	125	150	80	2
F2P1	140	800	40	2.5	32	125	150	80	2

Based on Table 15 and knowing that these panels were under shear stress and negative bending moment, the concrete contribution decreases due to its cracking, leading to a lower M_{pn} and distance between plastic hinges C resulting in a smaller contribution V_s. For such case the models ML1 and ML2 should not be used. In this case, under hogging moment, the model M4 present in EC3-1-5 correctly evaluates the ultimate shear resistance with an experimental/model ratio of about 1.01. According to Lääne [30], the slab contribution under negative moment is less than 10% of the steel girder's shear resistance.

Table 15 – Experimental and model results for CT4 composite girders

G	$V_{experimental}$ (kN)	V_{M4} (kN)	V_{ML1} (kN)	V_{ML2} (kN)	$V_{experimental}/V_{M4}$	$V_{experimental}/V_{ML1}$	$V_{experimental}/V_{ML2}$
F1P3	650.0	626.4	990.4	832.3	1.04	0.66	0.78
F1P5	605.0	587.8	814.8	713.1	1.03	0.74	0.85
F2P1	542.0	573.2	726.1	760.8	0.95	0.75	0.81

For the 4 Composite Tests analysed the results between both ML1 and ML2 models were somehow expected because both evaluates V_s part based on Cardiff Model, differing on

the fact that ML1 calculates V_c by ACI 318M-05 [31] and ML2 by EC2-1-1 [26]. In any case, these models are not so accurate to predict tests results, which is understandable given the number of parameters involved in such evaluation.

6. Case study

Located in Equatorial Guinea [32], the case study is a steel-concrete composite bridge with three spans 21.0+38.0+21.0 m with the characteristics shown in *Figure 4.* The overall view is presented in Figure 12.

The sections analysed in case study were a steel S355 NL end panel (S1) with a=5800 mm (M=0), intermediate support (S2) with a=2535 mm (M^-) and an intermediate panel (S3) with a=7602 mm (M^+). For each section an equivalent height and effective width of the slab were calculated. C30/37 concrete grade was used along with 4 shear connectors rows with D_n=40 mm, h_n=175 mm, transversal spacing of s=150 mm and longitudinal equivalent spacing of l=330 mm.

Figure 12 – Overall view of case study

According to Table 16, it is possible to conclude that, based on ML1 and ML2 results, the overall contribution of the composite action for the end support shear resistance is about 30% for both the intermediate panel and the end panel when compared with the results obtained from model M4, that only considers the steel girder shear resistance, used for the design of this bridge deck.

Table 16 – Ultimate shear resistance V_R for each model

Panel	V_{M1} (kN)	V_{M2} (kN)	V_{M3} (kN)	V_{M4} (kN)	V_{ML1} (kN)	V_{ML2} (kN)
S1	4322.2	4227,1	4340.6	4445.7	5598.8	5859.6
S2	5474.5	5388.7	4879.3	4658.9	-	-
S3	4093.7	4010.5	4283.6	4284.2	5516.2	5603.5

7. Conclusions

After analysing four different models to estimate the shear resistance of steel girders and two models for composite girders, and comparing both with experimental results, the main conclusions of this study are:

• The model M4 is the most accurate in order to evaluate the shear strength of steel plate girders, being also very simple and having large applicability;

• Despite currently ignored in norms, the shear resistance contribution of the non-cracked slab exists and may be considered in order to attain an optimized structural design;

• This compressed slab contribution may be traduced by an increase of 30 to 60% of steel girders shear resistance, being the average contribution about 50% for those beams studied. Under tension, the slab cracked contribution is under 10%, being conservative to disregard it.

8. Notation

a	Transverse stiffeners spacing
b_f	Width of the flange ($_b$ and $_t$ for bottom and top)
b_s	Width of the slab
c	Distance between plastic hinges (M4)
C_c	Distance between plastic hinges in comp. flange
C_t	Distance between plastic hinges in tens. flange
d	Height of the web
d_s	Effective height of the slab
D_n	Head diameter of shear connector
E	Young Modulus ($_w$ for web)
f_y	Yield tension of steel ($_f$ for flange, $_w$ for web)
f'$_c$	Compressive strength of concrete
f_{ck}	Characteristic compressive strength of concrete
f_{ctm}	Average tension strength of concrete
F_{st}	Strength of compressed strut
g	Width of the tension field membrane
h	Height of steel plate girder
h_n	Height of shear connector
k_τ	Shear buckling coefficient for the web panel
l	Longitudinal spacing of shear connectors
L	Span
L_e	Effective Span
M_{Ed}	Bending moment
$M_{f,Rd}$	Plastic moment of the flange
M_{pn}	Plastic moment of the composite flange
$M_{Nf,Rk}$	Characteristic plastic moment of the flange
N_{st}	Row numbers of shear connectors
t_f	Thickness of the flange
t_w	Thickness of the web
V_a	Concrete strength according to EC2
V_b	Pull-out capacity of the shear connectors
V_c	Concrete shear strength (^{B} for region-B, ^{D} for region-D)
V_R	Ultimate shear capacity of a plate girder
V_s	Steel girder shear strength
V_σ	Post-buckled shear strength (M1)
V_{cr}	Critical shear resistance
$V_{ba,Rk}$	Shear strength of steel girder (M3)
$V_{bb,Rk}$	Shear strength of steel girder (M2)
$V_{bf,Rd}$	Shear strength contribution of flanges (M4)
$V_{bw,Rd}$	Shear strength of the steel girder web (M4)
γ_M	Safety coefficient ($_0$ or $_1$)
η	Corrective coefficient (M4)
θ	Web panel diagonal inclination
$\bar{\lambda}_w$	Normalized slenderness of the web
ξ	Degree of interaction
σ_t	Tension in diagonal membrane (Von Mises)
τ	Tension in diagonal ($_{ba}$ for M3 and $_{bb}$ for M2)
τ_y	Design wield tension ($_w$ for web)
τ_{cr}	Critical tension of the web
χ_w	Reduction factor of web resistance
φ	Tension field inclination
ω	Strut inclination

9. References

[1] A. J. Reis e J. O. Pedro, "Railway Installation on the Tagus Suspension Bridge in Lisbon," *IABSE,* pp. 529-534, 1995.

[2] A. J. Reis e L. G. Melo, "Composite plate girder bridges: safety and serviceability," *IABSE conference,* pp. 235-240, 1997.

[3] A. J. Reis e N. T. Lopes, "Two Large Span Roofs for EURO 2004 Football Stadiums: Design and Erection," *Eurosteel conference,* 2005.

[4] A. J. Reis e N. T. Lopes, "Variante de Alcácer do Sal Atravessamento Ferroviário sobre o Rio Sado – Projecto de Obra de Arte," *VII Congresso de Construção Metálica e Mista,* 2009.

[5] F. Virtuoso, *Dimensionamento de Estruturas Metálicas: Vigas de Alma Cheia,* Lisboa: Elementos de apoio da Disciplina de Estruturas Metálicas do IST, 2009.

[6] S. F. Stiemer, *Advanced Structural Steel Design,* 2012.

[7] P. M. Mendes e J. O. Pedro, *Vigas de aço de secção soldada,* Lisboa: Elementos de apoio da Disciplina de Estruturas Especiais do IST, 2016.

[8] P. Esteves, *Tabuleiros de pontes híbridas aço/betão – Modelos de dimensionamento para regiões de ligação,* Lisboa: Tese de Mestrado em Engenharia Civil, IST, 2015.

[9] A. Reis e D. Camotim, Estabilidade e Dimensionamento de Estruturas, 1ª ed., Lisboa: Edições Orion, 2012.

[10] ENV 1993-1-1, *Eurocode 3: Design of Steel Structures - Part 1-1 General rules and rules for buildings,* European Committee of Standardization, 1992.

[11] NP EN 1993-1-5, *Eurocode 3: Design of Steel Structures - Part 1-5 Plated structural elements,* European Committee of Standardization, 2006.

[12] J. P. Lebet e M. A. Hirt, Steel Bridges Conceptual and Structural Design of Steel and Steel-Concrete Composite Bridges, Suiça: EPFL Press, 2013.

[13] NP EN 1993-1-1, *Eurocode 3: Design of Steel Structures - Part 1-1 General rules and rules for buildings,* European Committee of Standardization, 2010.

[14] C. M. M. Gomes, *Pontes Mistas Concepção, Projecto, Execução e Investigação,* Braga, 1999.

[15] S. C. Lee e C. H. Yoo, "Experimental Study On Ultimate Shear Strength of Web Panels," *Journal of Structural Engineering,* pp. 838-846, 1999.

[16] N. E. Shanmugam e K. Baskar, "Steel–Concrete Composite Plate Girders Subject to Shear," *Journal of Structural Engineering,* pp. 1230-1242, 2003.

[17] R. P. Johnson e D. Anderson, Designer's Handbook to Eurocode 4, London: Thomas Telford, 1993.

[18] R. W. Allison, R. P. Johnson e I. M. May, "Tension-field acton in composite plate girders," *Proc. Institute Civil Engineering,* nº 73 Part 2, pp. 255-276, 1982.

[19] D. M. Porter e Z. A. E. Cherif, "Ultimate shear strength of thin webbed steel and concrete composite girders. Proc. Intl. Conf. on Steel and Aluminium Structures," *Composite Steel Structures: Advances, design and construction,* pp. 55-64, 1987.

[20] R. Narayanan, R. I. M. Al-Amery e T. M. Roberts, "Shear strength of composite plate girders with rectangular web cutouts," *Journal of Constructional Steel Research,* nº 12 Part 2, pp. 151-166, 1989.

[21] T. M. Roberts e R. I. M. Al-Amery, "Shear Strength of Composite Plate Girders With Web Cutouts," *Journal of Structural Engineering,* pp. 1897-1910, 1991.

[22] S. F. Darehshouri, N. E. Shanmugam e S. A. Osman, "Collapse Behavior of Composite Plate Girders Loaded in Shear," *Journal of Structural Engineering,* pp. 318-326, 2012.

[23] A. Hayatdavoodi e N. E. Shanmugam, "Web Buckling and Ultimate Strength of Composite Plate Girders Subjected to Shear and Bending," *International Journal of Structural Stability and Dynamics,* 2015.

[24] Yatim, M. Y. M., Shanmugam, N. E., Wan Badaruzzman, W. H., "Thin-Walled Structures: Tests of partially connected composite plate girders," *Elsevier,* pp. 13-28, 2015.

[25] D. M. Porter, K. C. Rockey e H. R. Evans, "The collapse behavior of plate girders loaded in shear," *Structural Engineering ,* nº 53 (8), pp. 313-325, 1975.

[26] NP EN 1992-1-1, *Eurocode 2: Design of concrete structures - Part 1-1: General rules and rules for buildings,* European Committee for Standardization, 2010.

[27] NP EN 1994-2, *Eurocode 4: Design of composite steel and concrete structures - Part 2: General rules and rules for bridges,* European Committee for Standardization, 2005.

[28] L. Calado e J. Santos, em *Estruturas Mistas de Aço e Betão*, Lisboa, IST Press, 2013, pp. 264-271.

[29] A. Blanc e M. G. Navarro, *Poutres mixtes à âme mince avec béton de fibres métalliques,* Lousanne: Tese de Mestrado em Engenharia Civil, EPFL, 1999.

[30] A. Lääne, *Post-Critical Behaviour of Composite Brigdes Under Negative Moment and Shear,* Suíça: Tese de Douturamento em Engenharia Civil, EPFL, 2003.

[31] ACI318M-05, "Building Code Requirement For Structural Concrete," *Copyright American Concrete Institute,* 2005.

[32] GRID International, *Projeto de Execução das pontes OA18 e OA19 (Peças desenhadas),* 2013-14.

[33] L. S. Silva e H. Gervásio, Manual de Dimensionamento de Estruturas Metálicas: Métodos Avançados Eurocódigo 3, Associação Portuguesa de Construções Metálicas e Mistas, 2007.

[34] S. Mamazizi, R. Crocetti e H. Mehri, "Numerical and experimental investigation on the post-buckling behavior of steel plate girders subjected to shear," *Proceedings of the Annual Stability Conference Structural Stability Research Council,* 2003.

[35] L. A. Lourenço, *Análise do efeito de redução de espessura no comportamento de vigas de inércia variável com secção em I,* Braga: Tese de Mestrado em Engenharia Civil, Universidade do Minho, 2005.

[36] Q. Q. Liang, B. Uy, M. A. Bradford e H. R. Ronagh, "Ultimate strength of continuous composite beams in combined bending and shear," *Journal of Constructional Steel Reserch,* 2004.

[37] S. C. Lee e C. H. Yoo, "Shear, Strength of Plate Girder Web Panel Under Pure," *Journal of Structural Engineering,* pp. 184-194, 1998.

[38] D. Lam, T. C. Ang e S. P. Chiew, Structural Steelwork-Design To Limit State Theory, 3ª ed., Inglaterra: Elsevier, 2004.

[39] J. A. T. Guimarães, *Análise e dimensionamento de pórticos mistos aço-betão,* Porto: Tese de Mestrado em Engenharia Civil, FEUP, 2009.